University of Groningen

# Consequences of Mrp2 deficiency for diclofenac toxicity in the rat intestine ex vivo

Niu, Xiaoyu; de Graaf, Inge A. M.; van de Vegte, Dennis; Langelaar-Makkinje, Miriam; Sekine, Shuichi; Groothuis, Geny M. M.

**IMPORTANT NOTE: You are advised to consult the publisher's version (publisher's PDF) if you wish to cite from it. Please check the document version below.**

*Document Version*
Publisher's PDF, also known as Version of record

Link to publication in University of Groningen/UMCG research database

# Consequences of Mrp2 deficiency for diclofenac toxicity in the rat intestine *ex vivo*

Xiaoyu Niu [a], Inge A.M. de Graaf [a,*], Dennis van de Vegte [a], Miriam Langelaar-Makkinje [a], Shuichi Sekine [b], Geny M.M. Groothuis [a]

[a] *Division of Pharmacokinetics, Toxicology and Targeting, Department of Pharmacy, University of Groningen, The Netherlands*
[b] *Biopharmaceutics, Graduate School of Pharmaceutical Sciences, Chiba University, Japan*

### ABSTRACT

The non-steroidal anti-inflammatory drug diclofenac (DCF) has a high prevalence of intestinal side effects in humans and rats. It has been reported that Mrp2 transporter deficient rats (Mrp2−) are more resistant to DCF induced intestinal toxicity. This was explained *in vivo* by impaired Mrp2-dependent biliary transport of DCF-acylglucuronide (DAG), leading to decreased intestinal exposure to DAG and DCF. However, it is not known to what extent adaptive changes in the Mrp2− intestine itself influence its sensitivity to DCF toxicity without the influence of liver metabolites. To investigate this, DCF toxicity and disposition were studied *ex vivo* by precision-cut intestinal slices and Ussing chamber using intestines from wild type (WT) and Mrp2− rats. The results show that adaptive changes due to Mrp2 deficiency concerning Mrp2, Mrp3 and BCRP gene expression, GSH content and DAG formation were different between liver and intestine. Furthermore, Mrp2− intestine was intrinsically more resistant to DCF toxicity than its WT counterpart *ex vivo*. This can at least partly be explained by a reduced DCF uptake by the Mrp2− intestine, but is not related to the other adaptive changes in the intestine. The extrapolation of this data to humans with MRP2 deficiency is uncertain due to species differences in activity and regulation of transporters.

© 2014 Elsevier Ltd. All rights reserved.

## 1. Introduction

Diclofenac (DCF) is a non-steroidal anti-inflammatory drug (NSAID), which is frequently prescribed for the treatment of acute injury pain, postoperative pain, rheumatoid arthritis and osteoarthritis due to its excellent analgesic and anti-inflammatory properties (Small, 1989). However, clinical use of DCF has been associated with a high prevalence of intestinal side effects, as up to 70% of the patients developed intestinal injury while receiving DCF therapy

(Davies et al., 2000). DCF-induced intestinal injury was also found in rats, where DCF induced multiple ulcers and erosions in the small intestinal mucosa (Goncalves Junior et al., 2012).

It has been reported that Mrp2 deficient rats are more resistant to diclofenac-induced intestinal toxicity than their WT counterparts. The reduced toxicity has been suggested to be related to the impaired biliary transport of diclofenac acyl-glucuronide (DAG) into the intestine, since DAG is one of the substrates of the Mrp2 transporter (Seitz and Boelsterli, 1998; Seitz et al., 1998). Entero-hepatic circulation is an important determinant of DCF intestinal toxicity *in vivo*. Firstly, the intestine is exposed to the potentially harmful DAG metabolites. These electrophilic metabolites are produced in the liver and excreted across the canalicular membrane reaching high concentrations in the bile, leading to high intestinal exposure and therefore electrophile stress (LoGuidice et al., 2012; Treinen-Moslen and Kanz, 2006). Secondly, the DAG metabolites are deconjugated in the intestine by bacteria and the aglycone DCF is taken up again by the enterocytes (LoGuidice et al., 2012). Thus, the entero-hepatic cycling prolongs the intestinal exposure to DAG and its deconjugated DCF aglycone.

The ABC transporter Mrp2, a member of an exporter family that is expressed in hepatocytes, enterocytes, renal tubules and other

epithelial cells (Jedlitschky et al., 2006), plays a crucial role in the entero-hepatic circulation of DCF. In the liver, it is localized in the canalicular membrane of the hepatocytes where it transports endogenous compounds, drugs and their metabolites (such as DAG) into the bile (Keppler et al., 1997). The deficiency of Mrp2 results in a reduced biliary transport of DAG into the intestine. Since Mrp2 is also located in the intestine, where it is expressed in the brush-border membrane as an efflux transporter facilitating secretion of substrates back into the intestinal lumen (Mottino et al., 2000). The deficiency of Mrp2 in the intestine itself may result in changes of intestinal disposition of DCF, therefore influencing DCF intestinal toxicity directly. Moreover, Mrp2 has a broad range of substrates, not only drug glucuronide conjugates, but also glutathione, leukotrienes, bilirubin glucuronides, conjugated bile salts and drug sulfate conjugates (Treinen-Moslen and Kanz, 2006). As a result, except for reduced biliary export of DAG into the intestine, several adaptive changes have been found in the Mrp2$^-$ rat liver, such as less biliary export of GSH (Elferink et al., 1989), up-regulation of Mrp3 expression (Xiong et al., 2002), decreased Cytochrome P 450 (CYP) (Oguro et al., 1996) and increased UDP-glucuronosyltransferase (UGT) activity (Nishino et al., 2000). Some of these adaptive changes also occurred in the intestine (Johnson et al., 2006), but very limited studies were performed, and it is not clear to which extent these changes in the intestine influence the intestinal response to the DCF toxicity.

For this reason, in the present report we studied the consequences of Mrp2 deficiency in the rat intestine by two *ex vivo* preparations that allow studying the intestinal toxicity under conditions that exclude the influence of the liver. Two rat strains that lack a functional Mrp2 transporter, the Wistar-derived TR$^-$ (transporter deficient) rat and the Sprague–Dawley (SD) derived EHBR (eisai hyperbilirubinemic) rat were compared with their wild type controls (Ito et al., 1997; Paulusma et al., 1996). Precision-cut tissue slices of the liver and intestine (Wistar and TR$^-$ rats) were used to investigate the consequences of the Mrp2 deficiency related changes on Mrp3, Mrp2 and BCRP expression, DCF metabolism, GSH content and the resulting sensitivity of the intestine to DCF toxicity. Recently we have shown that this *ex vivo* model adequately reflects the NSAID-induced toxicity in human (Niu et al., 2014a) and rat PCIS (Niu et al., 2014b). In addition, the Ussing Chamber set-up (SD and EHBR rats) was used to compare absorption, transport and metabolism of DCF between the Mrp2 deficient rat intestine and the wild type rat intestine.

## 2. Materials and methods

### 2.1. Animals

Male Groningen-Yellow transporter-deficient rats were obtained from the Radboud University of Nijmegen (The Netherlands). Their wild type counterparts, male Wistar rats, were obtained from Charles River (Sulzfeld, Germany). The rats (weighing 250–350 g) were kept in a temperature- and humidity-controlled room with a 12 h light/dark cycle and free access to food (Harlan chow No. 2018, Harlan Laboratories BV, Horst, The Netherlands) and tap water. The Animal Ethics Committee of the University of Groningen approved the experiments with both types of rats. Precision cut tissue slices were obtained from these rats in The Netherlands.

Male Eisai hyperbilirubinemic rats and their wild type counterpart, Sprague Dawley rats, (weighing 240–300 g) were obtained from Japan SLC Inc. (Shizuoka, Japan). The housing situation was similar to that used in Groningen. All procedures described were approved by the animal care committee of the Chiba University. Ussing Chamber experiments were performed with intestinal tissue from these rats in Japan.

### 2.2. Preparation of the precision-cut intestinal slices and liver slices

Precision-cut intestinal and liver slices were prepared as described in detail by de Graaf et al. (2010). In brief, rats were sacrificed under anesthesia with isoflurane/O$_2$. The intestine was stored in freshly made ice-cold oxygenated Krebs–Henseleit buffer (pH 7.4), and the liver was stored in ice-cold University of Wisconsin (UW) organ preservation solution (DuPont Critical Care, Waukegab, IL). Subsequently, the jejunum was washed, cut into 3 cm segments, filled with 3% low melting agarose (Sigma–Aldrich, St. Louis, MO, USA), embedded in 3% agarose using a tissue embedding unit. Intestinal slices with a thickness of 350 μm and a wet weight of 3 mg were sliced using a Krumdieck tissue slicer (Alabama R&D, Munford, AL, USA) and stored in ice-cold oxygenated Krebs–Henseleit buffer (pH 7.4) until further use. Liver cores with a diameter of 5 mm were made using an electrical drill with a tissue coring tool. The cylindrical cores were subsequently sliced using a Krumdieck tissue slicer producing slices with a thickness of 250 μm and a wet weight of 5 mg. The slices were stored in the ice-cold UW until further use.

### 2.3. Incubation of the precision-cut slices

The slices were incubated individually in 12 wells plates (Greiner Bio-one GmbH, Frickenhausen, Austria) as described by de Graaf et al. (2010). Each well contained 1.3 ml Williams Medium E with Glutamax-I (Gibco, Paisley, UK) supplemented with 25 mM D-glucose (Merck, Darmstadt, Germany). 50 μg/ml gentamicin (Gibco, Paisley, UK) and 2.5 μg/ml fungizone (Gibco, Paisley, UK) was added only for the intestinal slices but not for the liver slices. The plates were placed in plastic boxes with shaking (90 times per minute) in an incubation cabinet at 37 °C, the medium was oxygenated by carbogen (95% O$_2$ and 5% CO$_2$), and the pH was kept at 7.4.

### 2.4. ATP determination

Viability of slices after 5 h of incubation with DCF (0–200 μM) was determined by measuring the ATP content according to the method described earlier (van de Kerkhof et al., 2006). In brief, three replicate slices were collected individually in 1 ml of 70% ethanol (v/v) containing 2 mM EDTA (pH 10.9) and snap-frozen in liquid nitrogen and stored at −80 °C until analysis. The intracellular ATP content of the slices was assessed using the ATP Bioluminescence Assay kit CLS II (Roche, Mannheim, Germany). The ATP content was corrected by the amount of protein of each slice and expressed as pmol/μg protein. The protein amount in the pellet remaining after ATP measurement was determined using the Bio-Rad DC Protein Assay (Bio-Rad, Munich, Germany) with bovine serum albumin (BSA, Sigma–Aldrich, Steinheim, Germany) as standard for the calibration curve.

### 2.5. Glutathione levels

Reduced glutathione (GSH) level was measured in the liver and the intestine, and compared between WT rats and Mrp2$^-$ rats. Details of this method were described by Hadi et al. (2012). In brief, fresh intestinal or liver slices were collected, washed in 0.9% NaCl solution, snap frozen in liquid nitrogen, stored at −80 °C until further use. Samples were homogenized in 400 μl 50 mM Tris–HCl/1 mM EDTA buffer (pH 7.4). 200 μl Ellman's reagent DTNB (5,5′-dithiobis-(2-nitrobenzoic acid)) (Sigma–Aldrich, St. Louis, MO, USA) was added into 50 μl sample supernatant, and the GSH concentration was determined by measuring the absorbance at 405 nm using spectrophotometric 96 wells plate

reader (Thermomax microplate reader, Molecular devices, Sunnyvale, CA, USA).

### 2.6. Gene expression

Fresh slices from intestine and liver were snap frozen in liquid nitrogen, and stored at $-80\,°C$ until further use. RNA was isolated with RNeasy Mini Kit (Qiagen, Hilden, Germany) according to the manufacturer's protocol.

The amount of RNA after isolation was measured with a Nanodrop ND-1000 Spectrophotometer (Nanodrop Technologies, Wilminton, DE, USA) at 230 nm. All RNA samples were diluted to a concentration of 2 ng/µl. From 0.5 µg RNA, cDNA was synthesized using the Promega Reverse Transcription System (Promega, Madison, WI, USA). The following solutions were added to 8.16 µl 2 ng/µl RNA: 10 µl $MgCl_2$ (25 mM), 2.5 µl 10× RT buffer, 2.5 µl dNTP's (10 mM), 0.8 µl random primers (0.5 µg/µl), 0.5 µl RNasin (40 U/µl) and 0.5 µl AMV-RT (25 U/µl). The samples were placed in a Mastercycle Gradient (Eppendorf AG, Hamburg, Germany) to start the cDNA synthesis with 1 cycle of 25 °C/10 min; 45 °C/60 min and 95 °C/5 min. Afterwards, the cDNA samples were stored at $-20\,°C$.

For RT-PCR, 1.25 µl cDNA was pipetted on a 384 wells real-time PCR plate (Applied Biosystems, Carlsbad, CA, USA). Subsequently, 18.8 µl of a mixture containing 0.4 µl forward primer (50 µM), 0.4 µl reverse primer (50 µM), 8 µl RNase free water and 10 µl SYBR Green mix (Abgene, Epsom, UK), was added to each sample. The plate was covered by an ADI PRISM Optical Adhesive Cover and centrifuged for 5 min at 2000 rpm. Samples were analyzed with a real-time PCR ABI PRISM© 7900HT Sequence Detection System according to the protocol for real-time PCR with SYBR Green using the SDS 2.4 software (Applied Biosystems, Carlsbad, CA, USA). The following primers were used:

GAPDH: 5′-CGCTGGTGCTGAGTATGTCG-3′; 3′-CTGTGGTCATGA GCCCTTCC-5′.
Mrp2: 5′-CTGGTGTGGATTCCCTTGG-3′; 3′-CAAAACCAGGAGCCA TGTGC-5′.
Mrp3: 5′-ACACCGAGCCAGCCATATAC-3′; 3′-TCAGCTTCACATTGC CTGTC-5′.
Bcrp: 5′-AATCAGGGCATCGATCTGTCA-3′; 3′-CAGGTAGGCAATT GTGAGGAA-5′.

To quantify the expression of the genes the comparative threshold cycle ($Ct$) was used. GAPDH was used as the housekeeping gene and the $Ct$ values of the other genes were corrected with the $Ct$ value of GAPDH ($\Delta Ct$). The $\Delta Ct$ of the $Mrp2^-$ rat tissue was then normalized to the $\Delta Ct$ of the wild type rat tissue ($\Delta\Delta Ct$). The fold difference was calculated by the formula: $2^{-\Delta\Delta Ct}$. The $Ct$ values of GAPDH were similar in the $Mrp2^-$ rat tissue and the WT rat tissue.

### 2.7. DCF metabolism in the slices

Intestinal or liver slices obtained from WT rats and $Mrp2^-$ rat were incubated with 50 µM DCF for 5 h. Medium was collected afterwards. 10 µl 2 M acetic acid (Merck, Darmstadt, Germany) was added to 500 µl medium to stabilize the metabolites, especially DAG which is labile in neutral and alkaline solution. 100 µl medium sample was injected into the HPLC. Samples were separated by a 5 µm Hypersil Gold column (150 × 4.6 mm) (Thermo Technologies, Bellefonte, PA, USA) with 25% acetonitrile/0.05 M ammonia formate (pH 6.2) as eluent, at a flow rate of 1.0 ml/min, during 30 min. Peaks were identified by a UV detector at 282 nm. DCF and its metabolites were identified by adding standard DCF, 4′-OH DCF, 5-OH DCF and DAG (Toronto research chemical Inc., Toronto, Canada) as the references and quantified using appropriate standard curves.

### 2.8. Ussing Chamber preparation

The Ussing Chamber protocol was adapted from a published method (Oga et al., 2013; Fortuna et al., 2012). Rats were sacrificed by cervical dislocation and the entire small intestine was rapidly removed, stored in the Krebs–Ringer buffer (KRB) solution, composed of 115 mM NaCl, 25 mM $NaHCO_3$, 2.4 mM $K_2HPO_4$, 1.2 mM $CaCl_2$, 1.2 mM $MgCl_2$, 0.4 mM $KH_2PO_4$, and 10 mM D-glucose, pH 7.4 saturated with carbogen (95% $O_2$, 5% $CO_2$). Jejunum was cut at a distance of 25–40 cm from the stomach, rinsed with ice-cold Krebs solution to remove the luminal contents and opened along the mesenteric border. 1.7 cm long segments, excluding visible Peyer's patches, were prepared and carefully mounted in NaviCyte Vertical Multichannel Ussing Chambers (Harvard Apparatus Inc., Holliston, MA, U.S.A.) with $0.64\,cm^2$ of exposed area. Each compartment was filled with 5 ml of KRB buffer supplemented with 10 mM D-glucose (pH 7.4) on the serosal side and 10 mM mannitol (pH 6.4) on the mucosal side of the jejunum tissue. The slightly acidic pH (pH 6.4) in the apical side represents the average pH in the lumen of the rat small intestine, whereas the neutral pH (pH 7.4) in the basolateral side mimics the pH of the blood. The tissue was kept at 37 °C during the experiments using a circulating water bath attached to a heat block, The incubation buffer was oxygenated with carbogen.

### 2.9. DCF permeation experiments in the Ussing Chamber

A stock solution (50 mM) of DCF sodium salt (Sigma–Aldrich, St. Louis, MO, USA) was made in dimethylsulfoxide (DMSO, Sigma–Aldrich, St. Louis, MO, USA) and kept at 4 °C in dark. Diclofenac sodium [carboxyl-$^{14}$C] was purchased from American Radiolabeled Chemicals. Inc. (0.1 mCi/ml, 55 mCi/mmol, 1.8 µmol/ml), and stored at $-20\,°C$ in the dark. After an equilibrium period of 30 min, the experiment was started by adding DCF (5 µl 50 mM stock solution plus 5 µl $^{14}$C-DCF) into the donor compartment to a final concentration of 50 µM and 0.1 µCi/ml $^{14}$C. Transport from mucosal to serosal (M–S) or from serosal to mucosal (S–M) was measured during 150 min by taking 500 µl samples from the receiver chamber every 30 min. An equal volume of pre-warmed blank buffer was added immediately after each sample was withdrawn to maintain a constant volume in the chamber.

Jejunum tissue integrity was observed throughout the experiment by measuring the inulin permeability. 200 µl [$^{14}$C] inulin (250 µCi/ml) was added alone or with DCF 50 µM in the donor compartment at pH 6.4 and pH 7.4. The radioactivity was measured every 30 min in the receiver compartment.

In the DCF experiments, the radioactivity accumulated in the mucosal tissue was measured at the end of the experiment. The mucosa was scraped from the part of the tissue that was exposed to the medium in the Ussing Chambers and homogenized in 400 µl 25% acetonitrile (ACN). After centrifugation (13,200 rpm, 5 min), 100 µl of the supernatant was used to measure the total tissue radioactivity and 100 µl was injected into the HPLC to measure the amount of metabolites in the tissue as described below.

To analyze the metabolites of DCF in the medium, 2.5 ml buffer in the receiving chamber was collected at the end of the experiment in glass tubes. 12.5 ml of ethyl acetate was added, the mixture was vortexed for 3 min. to extract the compounds from the aqueous phase. The tubes were stored at room temperature for 10 min, until the organic and the aqueous phase were fully separated. 12 ml was taken from the organic layer into a new tube and evaporated by nitrogen flow at room temperature using a speed vacuum system (SpeedVac®, RVA-400, Savant Instruments Inc., Holbrook, NY). Residuals were dissolved in 200 µl 25% ACN eluent, vortexed for 5 min to dissolve the residue and then 100 µl of this solution was injected into the HPLC.

The HPLC system was the same as that used in the slice metabolism studies, and was described in Section 2.7 above. A standard mixture of DCF, DAG, 4′-OH DCF and 5-OH DCF (Toronto research chemical Inc., Toronto, Canada) was injected into the HPLC for calibration. The retention time (min) for each of the compound were: 7.72 (4′-OH DCF), 8.92 (5-OH DCF), 12.02, 13.56, 15.6, 17.58, 22.87 (DAG and its isomers), and 25.54 (DCF). The eluent was collected in 1 ml fractions with a fraction collector (GE Healthcare Bio-Sciences KK, Kyoto, Japan) each minute and the samples were mixed with 2 ml of Clearsol I scintillation cocktail (Nacalai Tesque, Kyoto, Japan). The radioactivity was measured with a LSC-6100 liquid scintillation counter (Aloka, Tokyo, Japan). The fractions of 4′-OH DCF and 5-OH DCF were combined, and the radioactivity of the fractions of all the isomers of DAG was added together for the final calculation of DAG formation. The recovery of DCF, OH-DCF, DAG in buffer/ethyl acetate (1:5) was assessed to be 34%, 48%, 40% respectively, and the measured concentrations in the samples were corrected accordingly. The amount of DCF and its metabolites in the tissue and in the receiver compartment was calculated.

## 2.10. Statistics

Each experiment was performed with a minimum of three rats, using three PCIS or one Ussing Chamber for each experimental condition from each rat. Two-way ANOVA (mixed effect model) with Scheffée post hoc correction was used for the statistical analysis in Fig. 1, using SPSS 20.0 (IBM, Armonk, New York). Student t-test was used for Figs. 2–5 and Table 1. $P < 0.05$ was chosen to denote a significant difference between means.

# 3. Results

## 3.1. Intrinsic toxicity of DCF in wild type and Mrp2 deficient rat intestine

To investigate which part of the intestine was most sensitive, DCF induced toxicity along the rat intestine was studied using DCF 200 μM. This concentration showed toxicity in jejunum PCIS previously (Niu et al., 2014b). DCF induced more ATP decrease in rat jejunum slices (46% decrease) than in duodenum (23% decrease), ileum (25% decrease) and colon (10% decrease), which indicates that rat jejunum is more sensitive to DCF toxicity than the other three regions. Therefore we decided to use jejunum tissue to compare the toxicity in the wild type and the mutant rats.

Jejunum slices from wild type (WT) Wistar rats and Mrp2 deficient (Mrp2⁻) Wistar rats were incubated for 5 h with a range of concentrations of DCF (0–200 μM). The viability was determined based on the ATP concentrations in the slices. In accordance with our earlier observation (Niu et al., 2014b), DCF induced a concentration-dependent decrease of ATP in the slices from WT rats which reached statistical significance at 200 μM (44% decrease). In contrast, the ATP levels were not significantly changed at all concentrations in intestinal slices of the Mrp2⁻ rats (<22% decrease) (Fig. 1).

## 3.2. Comparison of Mrp2, Mrp3 and Bcrp gene expression in liver and intestine between WT and Mrp2⁻ rats

The gene expression of Mrp2, Mrp3 and Bcrp was measured in fresh liver and intestinal slices from WT and Mrp2⁻ rats respectively. The gene expression in wild type rats was normalized to one, and the fold difference was shown for the Mrp2⁻ rats. In the intestine, no significant difference was found between Mrp2⁻ rats and WT rats of the three genes tested (Fig. 2a). However, in the liver, a significantly lower Mrp2 and Bcrp gene expression and a higher Mrp3 gene expression were found in the Mrp2⁻ rats compared to WT rats (Fig. 2b).
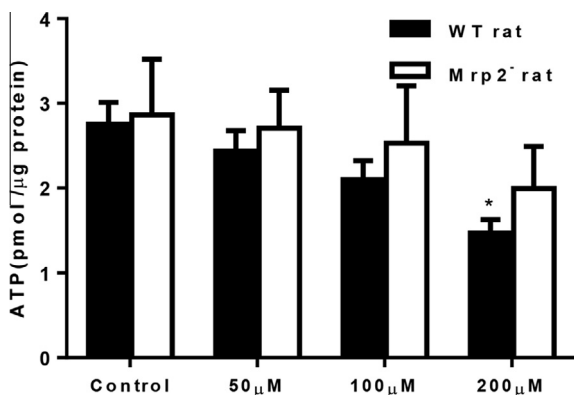


**Fig. 1.** Dose dependent toxicity of DCF in rat intestinal slices. DCF-induced decrease in ATP content in PCIS was compared between wild type rats (WT, black bars) and Mrp2 deficient rats (Mrp2⁻, white bars). The ATP content was corrected by the protein amount of each slice. Data represent the mean ± SEM ($n \geqslant 6$ rats). *Significantly different compared to control slices incubated for 5 h without DCF, $p < 0.05$ two-way ANOVA (mixed effect model) with Scheffée post hoc correction.
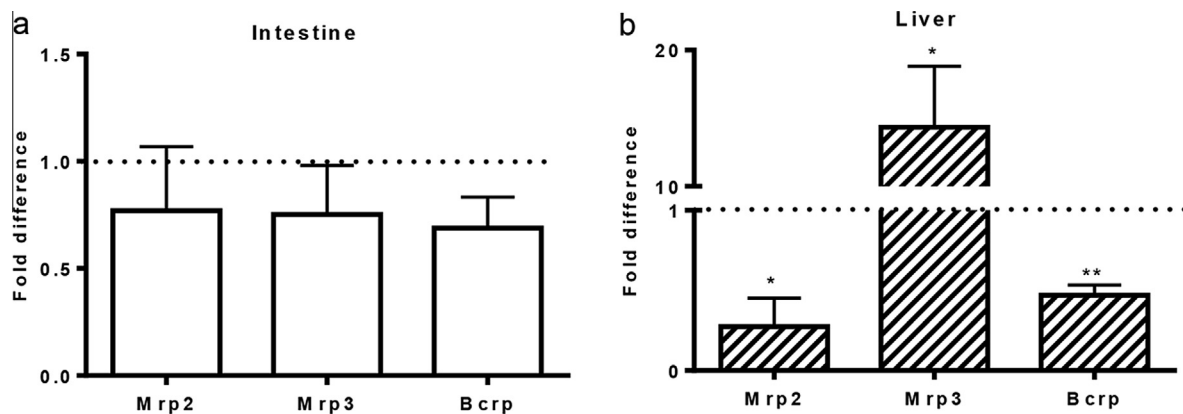


**Fig. 2.** Mrp2, Mrp3, Bcrp gene expression comparison. Gene expression in the intestine (a) and liver (b) was compared between Mrp2⁻ rats and WT rats. The gene expression in WT rats was normalized to one. The fold difference is shown for the Mrp2⁻ rats. Data represent the mean ± SEM ($n = 4$ rats). *Significantly different compared to WT rats, $p < 0.05$, Student t-test.
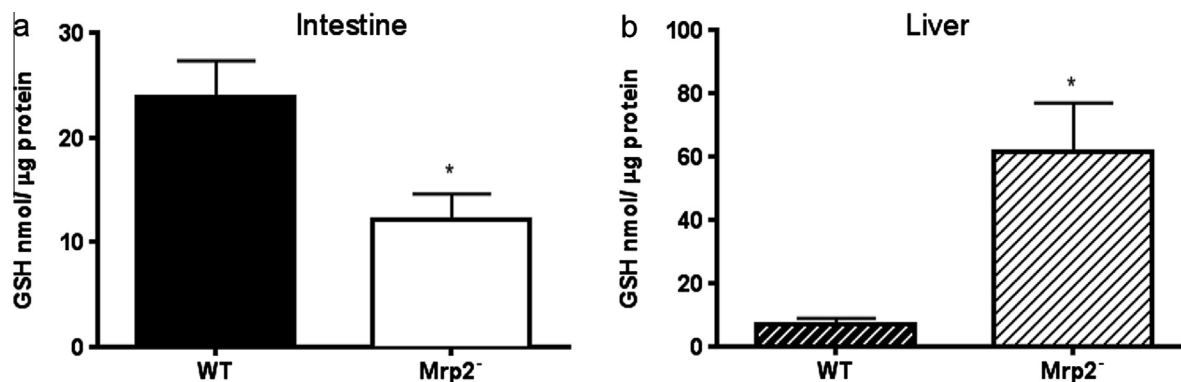
**Fig. 3.** Comparison of intracellular GSH level. GSH level in the intestine (a) and liver (b) was compared between WT and Mrp2⁻ rats. Data are presented as means ± SEM ($n \geqslant 3$ rats). *Significantly different compared to WT rats, $p < 0.05$, Student *t*-test.
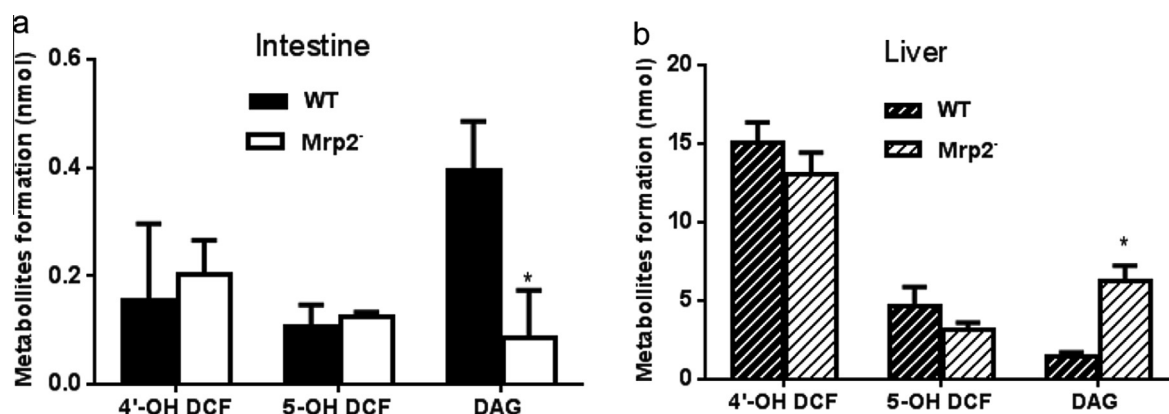


**Fig. 4.** DCF metabolism in WT and Mrp2⁻ intestinal and liver slices. DCF metabolites excreted after 5 h incubation in the medium by the intestinal (a) and liver (b) slices obtained from Mrp2⁻ rats and WT rats. Data are presented as mean ± SEM ($n = 3$ rats). *Significantly different compared to WT rats, $p < 0.05$, Student *t*-test.

### 3.3. Glutathione level

The intracellular GSH levels were measured in fresh liver and intestinal slices of WT and Mrp2⁻ rats. A significantly lower GSH level was found in the Mrp2⁻ rat intestine (12.1 ± 2.4 nmol/mg protein) than in the WT rat intestine (23.8 ± 3.4 nmol/mg protein) ($p < 0.05$) (Fig. 3a). However, 9 times more GSH was found in Mrp2⁻ rat liver (61.4 ± 15.5 nmol/mg protein) than in WT rat liver (6.8 ± 1.6 nmol/mg protein) (Fig. 3b).

### 3.4. DCF metabolism in precision cut tissue slices

In order to investigate whether the difference in toxic response to DCF between WT and Mrp2⁻ rats was the result of a difference in the rate of formation of metabolites, intestinal and liver slices from WT and Mrp2⁻ rats were incubated with 50 µM DCF for 5 h, thereafter the metabolites formed and excreted in the medium were measured. For this experiment a non-toxic dose of 50 µM was chosen, in order to avoid any influence of toxicity on the metabolic rate. Fig. 4 shows the formation of the DCF metabolites. Similar amounts of hydroxylated metabolites of DCF were excreted by WT rat intestinal slices (0.16 ± 0.14 nmol 4′-OH DCF and 0.11 ± 0.04 nmol 5-OH DCF) and Mrp2⁻ rat intestine (0.20 ± 0.03 nmol 4′-OH DCF and 0.13 ± 0.01 nmol 5-OH DCF). Significantly less DAG was found in the medium of Mrp2⁻ rat intestinal slices (0.09 ± 0.02 nmol) compared to WT rats (0.39 ± 0.09 nmol). As for the liver, no difference was found for the formation of phase I metabolites: 15.0 ± 1.3 nmol 4′-OH DCF

and 4.7 ± 1.2 nmol 5-OH DCF was excreted by one WT rat liver slice, whereas 13.1 ± 1.4 nmol 4′-OH DCF and 3.2 ± 0.4 nmol 5-OH DCF was excreted by one Mrp2⁻ rat liver slice. In contrast to the intestine, a significantly higher amount of DAG was found in the medium of Mrp2⁻ rat liver slices (6.2 ± 1.0 nmol) than that of WT rats (1.4 ± 0.2 nmol). In the slices, the amount of the metabolites was too low to be measured.

### 3.5. Bidirectional transport rate of DCF in the Ussing Chamber

Intestines from EHBR rats and their wild type counterpart SD rats were used to measure DCF transport in Ussing Chamber experiments. The bidirectional transport from the mucosal to the serosal compartment (M–S) or from the serosal to the mucosal compartment (S–M) was measured during 2.5 h incubation. To assess the integrity and viability of the jejunum tissue the permeability of ¹⁴C-inulin was monitored in separate Ussing Chambers. The results showed a linear transport rate of inulin in both directions (M–S and S–M) during 2.5 h incubation (results not shown). The inulin permeability was not influenced by the introduction of DCF at both pH 6.4 and pH 7.4.

50 µM ¹⁴C-DCF was added in either the mucosal compartment or the serosal compartment. The bidirectional transport of DCF was monitored during 2.5 h incubation (Fig 5). A greater permeation in the M–S direction (3.8% ± 0.5%) than the S–M direction (0.8% ± 0.2%) was found in WT rats, similarly, a greater permeation in M–S direction (1.7% ± 0.1%) than the S–M direction (0.4% ± 0.03%) was also found in Mrp2⁻ rats. Pilot experiments
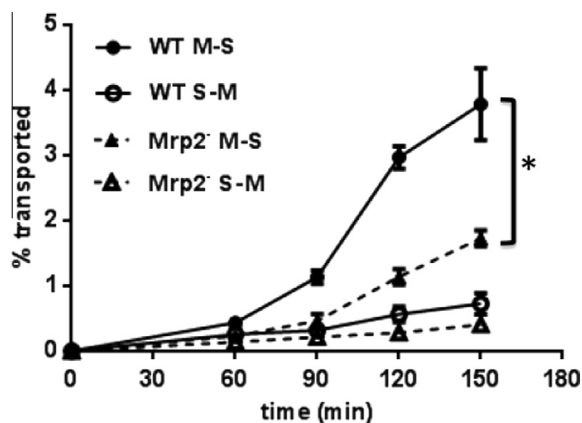
**Fig. 5.** Bi-directional transport of DCF in the Ussing Chamber study. Time profiles for the mucosal-to-serosal (M–S) and serosal-to-mucosal (S–M) flux of DCF and its metabolites in the jejunum of WT rats (solid line) and Mrp2− rats (dashed line). The experiments were initiated by adding DCF (50 μM) to the donor compartment. Radioactivity was measured in the receiving chamber, and expressed as the percentage of the initial amount added. Data represent the mean ± SEM ($n$ = 4 rats). *Significant difference between WT and Mrp2− rats, $p < 0.05$, Student $t$-test.

**Table 1**
Intestinal absorption and metabolism of DCF.

|  | 0 min Mucosal (nmol) | 150 min Tissue (nmol) | 150 min Serosal (nmol) | Total (nmol) |
|---|---|---|---|---|
| *WT (n = 4)* |  |  |  |  |
| DCF | 250 | 13.2 ± 1.6 | 11.1 ± 1.4 | 25.0 ± 2.0 |
| OH DCF | 0 | 0.2 ± 0.03 | 0.1 ± 0.004 | 0.2 ± 0.03 |
| DAG | 0 | 0.8 ± 0.1 | 0.4 ± 0.1 | 1.2 ± 0.1 |
| Total |  |  |  | 26.1 ± 2.0 |
| *Mrp2− (n = 4)* |  |  |  |  |
| DCF | 250 | 11.5 ± 1.8 | 4.9 ± 1.3* | 17.6 ± 2.2* |
| OH DCF | 0 | 0.1 ± 0.001 | 0.04 ± 0.01* | 0.1 ± 0.01 |
| DAG | 0 | 0.9 ± 0.3 | 0.1 ± 0.04* | 1.0 ± 0.5 |
| Total |  |  |  | 18.8 ± 2.3* |

DCF (250 nmol, 50 μM) was added into the mucosal compartment. The amount of DCF and its metabolites in the tissue and transported to the serosal compartment was examined after 2.5 h of incubation. Data represent the mean ± SEM ($n$ = 4 rats).
  * Significantly different from WT rats, $p < 0.05$, Student $t$-test.

with pH 6.4 or 7.4 in the mucosal compartment showed that this different permeation between M–S direction and S–M direction is not due to the lower pH in the mucosal compartment (6.4) (results not shown).

The intestine of the WT rats showed significantly higher permeability for DCF than Mrp2− rat intestine in M–S direction (Fig. 5), the total radioactivity recovered in the serosal compartment of WT rats (3.8% ± 0.5%) was more than two times higher than that of Mrp2− rats (1.7% ± 0.1%). However the difference in DCF permeability between WT and Mrp2− rats in the S–M direction was not significant.

### 3.6. DCF disposition in the Ussing Chamber experiments

When 250 nmol DCF was added in the 5 ml medium in the mucosal compartment, a similar amount of DCF was found in the tissue of the WT rat intestine (13.2 ± 1.6 nmol) and the Mrp2− rat intestine (11.5 ± 1.8 nmol) after 2.5 h incubation. However, much more DCF was transported into the serosal compartment by the WT rat intestine (11.1 ± 1.4 nmol) than that of Mrp2− rat intestine (4.9 ± 1.3 nmol). The total amount of DCF that was absorbed by the WT rat intestine (26.1 ± 2.0 nmol) was significantly higher than that absorbed by the Mrp2− rat intestine (18.8 ± 2.1 nmol) (Table 1).

With respect to the DCF metabolites, a similar amount of DAG was found in the tissue of the WT rat intestine (0.8 ± 0.1 nmol)

and the Mrp2− rat intestine (0.9 ± 0.3 nmol). However, significantly more DAG was transported into the serosal compartment by the WT rat intestine (0.4 ± 0.1 nmol) compared to the Mrp2− rat intestine (0.1 ± 0.04 nmol). A similar amount of OH-DCF was found in the tissue of WT rat intestine (0.15 ± 0.03 nmol) and the Mrp2− rat intestine (0.09 ± 0.001 nmol). More OH-DCF was transported into the serosal compartment by the WT rat intestine (0.14 ± 0.004 nmol) compared to the Mrp2− rat (0.04 ± 0.01 nmol).

## 4. Discussion

Mrp2 deficiency has previously been shown to attenuate diclofenac intestinal toxicity. This lower toxicity in Mrp2 deficient rat intestine was attributed to decreased excretion of DAG by Mrp2 from the liver into the intestine via the bile, leading to a lower exposure of the intestine to both this electrophilic metabolite (Seitz and Boelsterli, 1998; Seitz et al., 1998) and its deconjugated aglycone DCF (LoGuidice et al., 2012). In the present study, we examined the consequences of Mrp2 deficiency in the intestinal tissue *ex vivo* using precision-cut intestinal slices and the Ussing Chamber set-up, thereby excluding the influence of the liver-derived metabolites.

Our results show that the intestines of Mrp2− rats were intrinsically less sensitive to DCF toxicity than WT rat intestines. While 200 μM DCF reduced the ATP level significantly in WT rats (44% ± 7% decrease), this concentration was not sufficient to induce a statistically significant decrease of ATP in Mrp2− rat intestine (20% ± 6% decrease). This concentration of 200 μM DCF is a physiological relevant concentration as *in vivo* in rats, the ulcerogenic dose of DCF was reported to be 1.5–50 mg/kg body weight (Seitz and Boelsterli, 1998). Assuming a luminal volume of 11 ml (Davies and Morris, 1993), the *in vivo* luminal concentration can be estimated to be 0.1–3.6 mM, which is in the range of the *ex vivo* concentrations that were used in the present study. Also the incubation time is in accordance with the *in vivo* exposure time and is long enough to induce the toxicity (Niu et al., 2014b). Moreover because during this incubation time the non-exposed slices remain viable, and the amount of metabolites formed is only a fraction of the total amount of DCF added, it can be assumed that the metabolic rate is linear during 5 h. The intrinsically lower response to DCF in the Mrp2− rat intestine indicates that *in vivo*, in addition to the reduced exposure to biliary metabolites, some adaptive changes in the Mrp2− rat intestine itself contribute to its reduced sensitivity to DCF toxicity. Since Mrp2 is also expressed in the intestine (Suzuki and Sugiyama, 2002), the deficiency of Mrp2 could result in adaptive changes in other transporters which may modify the intestinal disposition of DCF, thereby influencing the sensitivity to DCF toxicity.

The Mrp2 mutation in the TR− rats is a single nucleotide deletion leading to a frame shift mutation and a stop codon. In EHBR rats, a one-nucleotide substitution results in a stop codon. These two rat strains have been extensively characterized, and both have no functional Mrp2 transporter (Ito et al., 1997; Paulusma et al., 1996). Diminished Mrp2 function, protein expression and gene expression was reported in the Mrp2 deficient rat liver (Paulusma et al., 1996). In the present study, using precision cut tissue slices, we confirmed that Mrp2 mRNA expression was significantly decreased in the Mrp2− rat liver when compared to the WT rats. This decrease in mRNA level as a result of a frame-shift mutation was tentatively explained by the increased break-down of the incomplete mRNA (Paulusma et al., 1996). In the intestine, surprisingly, no change in Mrp2 gene expression was observed in the present study, which was also reported by Ito et al. (1997). Previous studies have revealed, however, that the Mrp2 protein was indeed absent in the gut epithelial cells in Mrp2− rats (Johnson

et al., 2006), and the Mrp2 function was diminished as well (Gotoh et al., 2000).

A direct consequence of Mrp2 deficiency *in vivo* is a decreased biliary concentration and an increased plasma concentration of DAG, due to the Mrp2 dysfunction and increased expression of Mrp3 in the liver (Xiong et al., 2002). Up-regulation of Mrp3 is a well-known mechanism to compensate for the lack of Mrp2 function in the Mrp2⁻ rat liver (Xiong et al., 2002). Mrp3 is an efflux transporter localized at the basolateral surfaces of hepatocytes and enterocytes (Rost et al., 2002). It shares substrates such as glucuronide and glutathione conjugates with Mrp2 (Kruh et al., 2007). The up-regulation of Mrp3 facilitates extrusion of some Mrp2 substrates into blood and excretion via the urine when the Mrp2 is deficient. In the present study, we found that the Mrp3 expression in liver slices of Mrp2⁻ rats was 10 times higher than that in WT rats. However, no difference in Mrp3 expression was found in the intestine between WT rats and Mrp2⁻ rats. Similar observations were reported by Johnson (Johnson et al., 2006), who showed that the Mrp3 protein was significantly up-regulated in the liver and kidney of Mrp2⁻ rats, but was down-regulated in the small intestine. Since the up-regulation of Mrp3 in the liver was explained by its compensatory extrusion of accumulated Mrp2 substrates, the unchanged (down-regulated) Mrp3 in the intestine could indicate that Mrp2 substrates apparently do not accumulate in the Mrp2⁻ rat intestine, which is in line with the observation that the GSH content in the Mrp2⁻ rat intestine was not increased compared to the WT rat intestine in the present study.

As BCRP was also reported to be involved in the DCF disposition (Lagas et al., 2009), we investigated whether an increased BCRP expression could explain the reduced DCF toxicity in the intestine of the Mrp2⁻ rat. However, the data show no change in BCRP expression in the Mrp2⁻ rat intestine, which indicates that changes in the BCRP expression are unlikely to be the cause of the reduced intestinal toxicity in Mrp2⁻ rats. The Mrp2 deficiency resulted in a down-regulated BCRP gene expression in the liver in the present study, the reason remains unexplained up to now.

Differences in toxicity could also be the result of differences in metabolism of DCF. Indeed, an up-regulation of UGT2b1 and UGT1a in Mrp2⁻ rat liver was reported (Seitz et al., 1998; Nishino et al., 2000). Nevertheless, the DAG concentration in liver tissue in DCF-treated Mrp2⁻/⁻ mice was similar to that in WT mice (Lagas et al., 2010), indicating efficient compensatory transport by Mrp3. In the present study, a higher DAG concentration was found in the medium of Mrp2⁻ liver slices. In the slice system, both apical and canalicular excreted DAG will end up in the medium. Since decreased DAG transport by Mrp2 is thought to be compensated by Mrp3 activity and the net efflux is probably unchanged, the increased DAG in the medium is probably a result of an increased glucuronyl transferase activity in Mrp2⁻ rat liver. In the medium of the intestinal slices of Mrp2⁻ rats, less DAG was found in comparison to the WT rats. The Ussing Chamber experiments showed that DAG was not trapped in the intestinal tissue despite the fact that Mrp2 was absent and no compensatory up-regulation of Mrp3 was found in the Mrp2⁻ rat intestine. Taken together, this suggests that less DAG formation occurred in the Mrp2⁻ rat intestine. With respect to phase I metabolism, differential expression of CYP isoforms was also found in Mrp2⁻ rat microsomes compared to their corresponding non-mutant rats (Newton et al., 2005). However the data presented here indicate no difference in phase I metabolism.

Apart from the transport and accumulation of DCF metabolites, differences were also observed with respect to the disposition of DCF itself in the intestine. Firstly, a higher permeation of DCF from M–S direction was found than that of S–M direction in both rat strains (Fig. 5), which indicates the involvement of either an influx transporter in the apical membrane or an efflux DCF transporter in the basolateral side of the intestine. Secondly, a similar amount of DCF was found in the intestinal tissue of the WT and Mrp2⁻ rats, however, a larger amount of DCF was transported by the WT rat intestine than the Mrp2⁻ rats (Fig. 5, Table 1). Taken together, a larger amount of DCF was taken-up by the WT rat intestine than the Mrp2⁻ rats. This indicates that the DCF uptake in the enterocytes is possibly dependent on a transporter which is differentially expressed in the two rat strains. Even though we could not find any information which DCF transporter might be involved, the lower sensitivity of Mrp2⁻ rat intestine to DCF toxicity *ex vivo* and *in vivo* can at least partly be ascribed to its lower uptake of DCF. Moreover, this finding is in line with our previous results that DCF itself rather than its intestinal metabolites is responsible for the DCF intestinal toxicity (Niu et al., 2014a). The mechanistic explanation for the higher transport of DCF from M–S than S–M needs further research.

Changes in glutathione transport and metabolism are known to be another significant consequence of Mrp2 deficiency in the liver (Lu et al., 1996). Impaired extrusion of glutathione into the bile, and enhanced γ glutamylcysteine synthetase (γ-GCS) activity are considered to be responsible for the 5-fold increase in GSH content in Mrp2⁻ rat liver (Lu et al., 1996), which was also found in our studies using liver slices. In contrast to the liver, 50% less GSH was found in intestinal slices of Mrp2⁻ rats compared to WT rats. Since an important source of intestinal GSH is luminal GSH (Martensson et al., 1990) and biliary GSH is a major contributor to luminal GSH pool (Aw, 1994; Aw and Williams, 1992), one explanation for the reduced GSH in the intestine could be the blocked GSH transport via the bile into the intestine due to the Mrp2 deficiency in the liver. GSH is reported to detoxify the reactive hydroxyl DCF metabolites, and the reduced intracellular GSH level in the Mrp2⁻ rat intestine can be expected to lead to higher sensitivity to DCF toxicity. However, both previous *in vivo* studies and our results showed that DCF was less toxic to Mrp2⁻ rat intestine. The decreased GSH level in the Mrp2⁻ rat intestine did not render it more sensitive to DCF toxicity, which gives further indication that the intestinal DCF reactive hydroxyl metabolites are not responsible for its intestinal toxicity (Niu et al., 2014a).

In conclusion, we found that the intestine of Mrp2⁻ rats is intrinsically less sensitive to DCF-induced toxicity, which could at least partly be ascribed to its lower DCF uptake. Thus the reduced DCF intestinal toxicity found in the Mrp2⁻ rats *in vivo* is likely to be the result of both lower intestinal exposure to the liver-derived DAG (and its aglycone DCF) and a lower uptake of DCF. Moreover, we found that the consequences of Mrp2 deficiency with respect to transporter expression, GSH content and DCF metabolism are clearly different between the liver and intestine, but these consequences do not seem to be related to the reduced DCF toxicity in Mrp2⁻ rat intestine. Whether the findings can be extrapolated to human with a genetically deficient MRP2 is as yet uncertain, since the activity and regulation of transport proteins might be different in human and rat tissues.

## Conflict of Interest

The authors declare that there are no conflicts of interest.

## Transparency Document

The Transparency document associated with this article can be found in the online version.

# References

Aw, T.Y., 1994. Biliary glutathione promotes the mucosal metabolism of luminal peroxidized lipids by rat small intestine in vivo. J. Clin. Invest. 94, 1218–1225.

Aw, T.Y., Williams, M.W., 1992. Intestinal absorption and lymphatic transport of peroxidized lipids in rats: effect of exogenous GSH. Am. J. Physiol. 263, G665–G672.

Davies, B., Morris, T., 1993. Physiological parameters in laboratory animals and humans. Pharm. Res. 10, 1093–1095.

Davies, N.M., Saleh, J.Y., Skjodt, N.M., 2000. Detection and prevention of NSAID-induced enteropathy. J. Pharm. Pharm. Sci. 3, 137–155.

de Graaf, I.A., Olinga, P., de Jager, M.H., Merema, M.T., de Kanter, R., van de Kerkhof, E.G., Groothuis, G.M., 2010. Preparation and incubation of precision-cut liver and intestinal slices for application in drug metabolism and toxicity studies. Nat. Protoc. 5, 1540–1551.

Elferink, R.P., Ottenhoff, R., Liefting, W., de Haan, J., Jansen, P.L., 1989. Hepatobiliary transport of glutathione and glutathione conjugate in rats with hereditary hyperbilirubinemia. J. Clin. Invest. 84, 476–483.

Fortuna, A., Alves, G., Falcao, A., Soares-da-Silva, P., 2012. Evaluation of the permeability and P-glycoprotein efflux of carbamazepine and several derivatives across mouse small intestine by the Ussing chamber technique. Epilepsia 53, 529–538.

Goncalves Junior, I., Naresse, L.E., Rodrigues, M.A., Kobayasi, S., 2012. Diclofenac sodium and Imipenem action on rat intestinal mucosa: a biomechanical and histological study. Acta Cir. Bras. 27, 131–136.

Gotoh, Y., Suzuki, H., Kinoshita, S., Hirohashi, T., Kato, Y., Sugiyama, Y., 2000. Involvement of an organic anion transporter (canalicular multispecific organic anion transporter/multidrug resistance-associated protein 2) in gastrointestinal secretion of glutathione conjugates in rats. J. Pharmacol. Exp. Ther. 292, 433–439.

Hadi, M., Chen, Y., Starokozhko, V., Merema, M.T., Groothuis, G.M., 2012. Mouse precision-cut liver slices as an ex vivo model to study idiosyncratic drug-induced liver injury. Chem. Res. Toxicol. 25, 1938–1947.

Ito, K., Suzuki, H., Hirohashi, T., Kume, K., Shimizu, T., Sugiyama, Y., 1997. Molecular cloning of canalicular multispecific organic anion transporter defective in EHBR. Am. J. Physiol. 272, G16–G22.

Jedlitschky, G., Hoffmann, U., Kroemer, H.K., 2006. Structure and function of the MRP2 (ABCC2) protein and its role in drug disposition. Exp. Opin. Drug Metab. Toxicol. 2, 351–366.

Johnson, B.M., Zhang, P., Schuetz, J.D., Brouwer, K.L., 2006. Characterization of transport protein expression in multidrug resistance-associated protein (Mrp) 2-deficient rats. Drug Metab. Dispos. 34, 556–562.

Keppler, D., Konig, J., Buchler, M., 1997. The canalicular multidrug resistance protein, cMRP/MRP2, a novel conjugate export pump expressed in the apical membrane of hepatocytes. Adv. Enzyme Regul. 37, 321–333.

Kruh, G.D., Belinsky, M.G., Gallo, J.M., Lee, K., 2007. Physiological and pharmacological functions of Mrp2, Mrp3 and Mrp4 as determined from recent studies on gene-disrupted mice. Cancer Metastasis Rev. 26, 5–14.

Lagas, J.S., van der Kruijssen, C.M., van de Wetering, K., Beijnen, J.H., Schinkel, A.H., 2009. Transport of diclofenac by breast cancer resistance protein (ABCG2) and stimulation of multidrug resistance protein 2 (ABCC2)-mediated drug transport by diclofenac and benzbromarone. Drug Metab. Dispos. 37, 129–136.

Lagas, J.S., Sparidans, R.W., Wagenaar, E., Beijnen, J.H., Schinkel, A.H., 2010. Hepatic clearance of reactive glucuronide metabolites of diclofenac in the mouse is dependent on multiple ATP-binding cassette efflux transporters. Mol. Pharmacol. 77, 687–694.

LoGuidice, A., Wallace, B.D., Bendel, L., Redinbo, M.R., Boelsterli, U.A., 2012. Pharmacologic targeting of bacterial beta-glucuronidase alleviates nonsteroidal anti-inflammatory drug-induced enteropathy in mice. J. Pharmacol. Exp. Ther. 341, 447–454.

Lu, S.C., Cai, J., Kuhlenkamp, J., Sun, W.M., Takikawa, H., Takenaka, O., Horie, T., Yi, J., Kaplowitz, N., 1996. Alterations in glutathione homeostasis in mutant Eisai hyperbilirubinemic rats. Hepatol. 24, 253–258.

Martensson, J., Jain, A., Meister, A., 1990. Glutathione is required for intestinal function. Proc. Natl. Acad. Sci. U. S. A. 87, 1715–1719.

Mottino, A.D., Hoffman, T., Jennes, L., Vore, M., 2000. Expression and localization of multidrug resistant protein mrp2 in rat small intestine. J. Pharmacol. Exp. Ther. 293, 717–723.

Newton, D.J., Wang, R.W., Evans, D.C., 2005. Determination of phase I metabolic enzyme activities in liver microsomes of Mrp2 deficient TR- and EHBR rats. Life Sci. 77, 1106–1115.

Nishino, A., Kato, Y., Igarashi, T., Sugiyama, Y., 2000. Both cMOAT/MRP2 and another unknown transporter(s) are responsible for the biliary excretion of glucuronide conjugate of the nonpeptide angiotensin II antagonist, telmisaltan. Drug Metab. Dispos. 28, 1146–1148.

Niu, X., de Graaf, I.A., Langelaar-Makkinje, M., Horvatovich, P., Groothuis, G.M., 2014a. Diclofenac toxicity in human intestine ex vivo is not related to the formation of intestinal metabolites. Arch. Toxicol. (in press).

Niu, X., de Graaf, I.A., van der Bij, H.A., Groothuis, G.M., 2014b. Precision cut intestinal slices are an appropriate ex vivo model to study NSAID-induced intestinal toxicity in rats. Toxicol. In Vitro 28, 1296–1305.

Oga, E.F., Sekine, S., Horie, T., 2013. Ex vivo and in vivo investigations of the effects of extracts of *Vernonia amygdalina*, *Carica papaya* and *Tapinanthus sessilifolius* on digoxin transport and pharmacokinetics: assessing the significance on rat intestinal P-glycoprotein efflux. Drug Metab. Pharmacokinet. 28, 314–320.

Oguro, T., Kaneko, E., Kaneko, Y., Numazawa, S., Imaoka, S., Funae, Y., Mikami, T., Yoshida, T., 1996. Suppressed expression of phenobarbital-inducible hepatic cytochrome P-450s in Eisai-hyperbilirubinuria rats (EHBR/Eis). J. Pharmacol. Exp. Ther. 277, 1676–1684.

Paulusma, C.C., Bosma, P.J., Zaman, G.J., Bakker, C.T., Otter, M., Scheffer, G.L., Scheper, R.J., Borst, P., Oude Elferink, R.P., 1996. Congenital jaundice in rats with a mutation in a multidrug resistance-associated protein gene. Science 271, 1126–1128.

Rost, D., Mahner, S., Sugiyama, Y., Stremmel, W., 2002. Expression and localization of the multidrug resistance-associated protein 3 in rat small and large intestine. Am. J. Physiol. Gastrointest. Liver Physiol. 282, G720–G726.

Seitz, S., Boelsterli, U.A., 1998. Diclofenac acyl glucuronide, a major biliary metabolite, is directly involved in small intestinal injury in rats. Gastroenterology 115, 1476–1482.

Seitz, S., Kretz-Rommel, A., Oude Elferink, R.P., Boelsterli, U.A., 1998. Selective protein adduct formation of diclofenac glucuronide is critically dependent on the rat canalicular conjugate export pump (Mrp2). Chem. Res. Toxicol. 11, 513–519.

Small, R.E., 1989. Diclofenac sodium. Clin. Pharm. 8, 545–558.

Suzuki, H., Sugiyama, Y., 2002. Single nucleotide polymorphisms in multidrug resistance associated protein 2 (MRP2/ABCC2): its impact on drug disposition. Adv. Drug Deliv. Rev. 54, 1311–1331.

Treinen-Moslen, M., Kanz, M.F., 2006. Intestinal tract injury by drugs: importance of metabolite delivery by yellow bile road. Pharmacol. Ther. 112, 649–667.

van de Kerkhof, E.G., Ungell, A.L., Sjoberg, A.K., de Jager, M.H., Hilgendorf, C., de Graaf, I.A., Groothuis, G.M., 2006. Innovative methods to study human intestinal drug metabolism in vitro: precision-cut slices compared with ussing chamber preparations. Drug Metab. Dispos. 34, 1893–1902.

Xiong, H., Suzuki, H., Sugiyama, Y., Meier, P.J., Pollack, G.M., Brouwer, K.L., 2002. Mechanisms of impaired biliary excretion of acetaminophen glucuronide after acute phenobarbital treatment or phenobarbital pretreatment. Drug Metab. Dispos. 30, 962–969.